Influence of DNA Structure on the Reactivity of the Guanine Radical Cation

Francesco Luigi Gervasio,* Alessandro Laio, Marcella Iannuzzi, and Michele Parrinello[a]

Abstract: Oxidative damage of DNA via radical cation formation is a common cause of mutagenesis, cancer and of the physiological changes associated with aging. By using state-of-the-art ab initio molecular dynamics simulations, we study the mechanism that guides the first steps of this process. In the mechanism proposed here, guanine, which among the bases has the lowest oxidation potential, and the phosphate backbone play a crucial role. We found that the rate limiting step is the water protolysis. We illuminate the role of the local environment in considerably lowering the barrier. Of particular relevance in this respect is the role of the phosphate backbone.

Keywords: charge transfer · DNA · molecular dynamics · nucleic acids · oxidation

Introduction

Oxidative damage to DNA is a common event that through the formation of strand breaks and nucleobase modifications may cause mutagenesis, cancer and is involved in aging.[1,2] Fortunately, cells possess defense mechanisms such as base excision repair and break repair enzymes, which correct such damages in order to maintain the integrity of the genome.[3]

Since the DNA molecule has an extraordinarily clever structural design, it is natural to wonder if also its electronic structure has evolved so as to steer environmental damage toward specific products that could be more easily recognized by repair enzymes.

A crucial role concerning the effect of oxidative damage is played by guanine (G), which has the lowest oxidation potential among the nucleic acid bases,[4] and within GG and GGG clusters its ionization potential is even lower.[5–8] Guanine radical cation ($G^{\bullet+}$) can be formed either by direct oxidation by a large variety of agents[9] or indirectly via hole migration.[10] Extensive experimental and theoretical investigations have been carried on this topic.[4,7,9,11–19]

In this work, by applying state of the art computational techniques that enable to overcome large energetic barriers[20,21] and to follow the time evolution of a very large system,[22] we elucidate the nature and the consequences of a radical defect in a hydrated DNA fiber. In particular we have addressed two main issues.

We first analyzed the protonation state of the guanine radical cation/cytosine pair ($G^{\bullet+}$:C). In aqueous solution the $G^{\bullet+}$ undergoes a rapid deprotonation, since its pK_a is 3.9,[23] which leads to the formation of deprotonated guanine radical ($G(-H)^{\bullet}$). Experiments have shown that the proton lost is the one attached to N^1 (see Figure 2).[23,24] This has been confirmed by calculations on $G^{\bullet+}$ that take into account solvent effects in a simplified manner.[25]

In DNA G is paired with C, and so it is not completely clear which is the protonation state of the pair. Some believe that comparing the pK_a of $G^{\bullet+}$ and C in water would give a good estimate of the oxidized basis pair protonation state.[26,27] Others instead deem the gas-phase acidity as a more relevant model for the DNA environment.[9] Clearly either points of view are partial and while it is generally accepted that the protonation state of the G:C radical cation pair in DNA is $G(-H)^{\bullet}:C(H)^{+}$ this point of view is not based on direct observation. We found that the protonation state of $G^{\bullet+}$:C in DNA is different from that found in gas phase and that the source of this difference are the geometrical constraints imposed by the DNA backbone on the relative positions of the bases. This result was obtained by extensive quantum mechanics/molecular mechanics (QM/MM) simulations and by applying a novel method that allows fast and precise calculation of free energy profiles.

Second we elucidate the fate of the $G^{\bullet+}$:C base pair. There is experimental evidence that the final fate of the $G^{\bullet+}$ depends on its environment, as the products found in water are a mixture of products (imidazolones and oxazolones) while in double helical DNA the oxidation leads to 8-oxo-7,8-dihydro-2′-deoxyguanosine (8-oxo-G).[9,28–31] This difference has been ascribed to the putatively different proton-

[a] Dr. F. L. Gervasio, Dr. A. Laio, Dr. M. Iannuzzi, Prof. Dr. M. Parrinello
Laboratory of Physical Chemistry, ETH Zürich, USI Campus
via Giuseppe Buffi 13, 6904 Lugano (Switzerland)
Fax: (+41) 091-913-8817
E-mail: fgervasi@phys.chem.ethz.ch

Supporting information for this article is available on the WWW under http://www.chemeurj.org/ or from the author.

DOI: 10.1002/chem.200400171

ation state of guanine as well as the base stacking.[31] If one of these two effects is more important in changing the G reactivity or if both are involved is unclear. The ab initio calculations made on the G:C radical cation pair in gas phase have shown that when the G is protonated the formation of 8-oxo-G is exothermic, while when the G is deprotonated the oxidation reaction is endothermic.[16] But it is not clear if these gas-phase calculations are relevant for the $G^{\bullet+}$ in double stranded DNA and water solution, even more so since recent pulse-radiolysis experiments performed on the G radical in solution at different pH values show that neither the neutral $G(-H)^{\bullet}$ radical nor the $G^{\bullet+}$ give rise to 8-oxo-G;[32] this questions the role of the protonation state in determining the oxidation products. Extensive analysis of the free energy surface as a function of many possible reaction coordinates shows that an important role is played by the phosphate backbone which lowers the barrier for the rate limiting step of the reaction, that is, the protolysis of a water molecule close to the G, by enhancing a charge (and radical) transfer from the $G^{\bullet}$ to it.

These findings demonstrate the importance of the DNA backbone in guiding the oxidation process toward the 8-oxo-G.[33]

The calculations are performed on a fully hydrated double strand DNA decamer, namely d(GpCpGpCpGpCpGpCpGpCp)[34] (see Figure 1). This system has the smallest primitive cell among the self-complementary nucleotide crystals that have been synthesized in the laboratory, and its atomic and electronic structure have already been thoroughly characterized via full ab initio optimizations.[18] Although not biologically active, it has all the ingredients of an active DNA, namely the double strand, the counter-ions and the solvation waters. Furthermore the tight packing of the DNA strands resembles the situation found in the genes.[35] All the simulations were performed with periodic boundary conditions.

On this system we performed both a fully ab initio calculation of the radical cation state (where all the 3960 valence electrons of the atoms in the elementary cell were treated explicitly) and mixed quantum mechanics/molecular mechanics (QM/MM) simulations. In this latter approach, the system is partitioned into two regions, described, respectively, at the density functional theory level and with a classical force field (see ref. [36] for details). Within the quantum region all calculations were performed in the framework of density functional theory using two different gradient-corrected exchange and correlation functionals (see ref. [37] for details) and Martins–Troullier pseudopotentials for the core electrons.[38] All the calculations were made with the CPMD code.[39]

Great attention has been devoted to quantify the errors induced by the QM/MM approach. The geometry, the HOMO–LUMO gap, the properties of the frontier orbitals and the energetics of protonation state were compared to those of the full ab initio calculation and for all these properties we found a good agreement between the two methods.[40]

The reactions that are the object of this study involve the transition over barriers of the order of tens of kcal mol^{-1}.

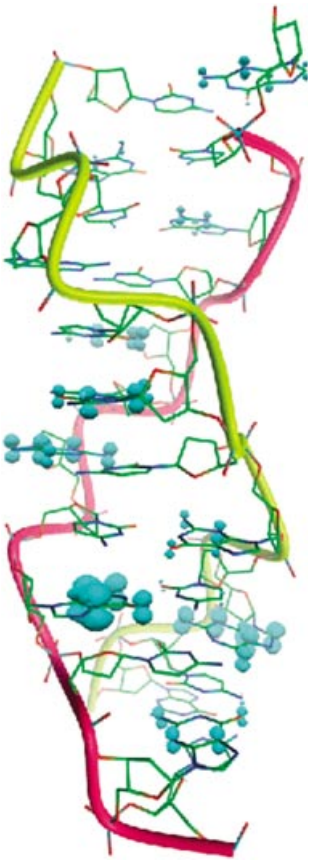

Figure 1. View of the three-dimensional structure of the G:C decamer d(GpCpGpCpGpCpGpCpGpCp) and of the spin density isosurface (in cyan) associated with the radical cation state. Water molecules, counterions and hydrogen atoms have been removed for clarity. The sugar-phosphate backbone is represented as tubes. Overall the elementary cell contains 654 heavy atoms and 540 hydrogen atoms (M_w $C_{228}N_{96}O_{144}P_{24}Na_{24}H_{264}\cdot 138\,H_2O$). The isosurface represented has a value of 10^{-3} electrons Å^{-3}.

This kind of activated process cannot be observed within the time scale of a full ab initio or even QM/MM simulations. In order to clear these barriers and reconstruct the free energy as a function of the relevant reaction coordinates, we apply the method already introduced in refs. [20,21] The method is based on a coarse-grained history-dependent dynamics (metadynamics) that is able to explore the free energy in the space defined by a manifold of collective coordinates S_α that characterize the reaction process. At each metadynamics step the system evolution is guided by the combined action of the thermodynamic force (which would trap the system in the free-energy wells) and a history-dependent force which disfavors configurations in S_α space that have already been visited. The history-dependent potential F_G, is constructed as a sum of Gaussians centred on each value of the S_α already explored during the dynamics. As shown,[20,21] F_G fills in time the minima in the free energy surface and, in the limit of a long metadynamics, the sum of F_G and F tends to become flat as a function of the S_α. As has been shown elsewhere,[20,21] meaningful results can be obtained in a relatively short simulation time if the S_α are able to discriminate between the initial and final state and include all the modes relevant to the reaction that cannot be sampled within the

typical time scale of an ab initio MD run. In the present work the S_α were chosen to be a combination of two or three coordination numbers.[41] and we use the metadynamics algorithm described in ref. [21] The coordination number is the number of atoms of one type (e.g. hydrogen atoms) at a bonding distance from another atom (e.g. G-N^1) and is defined as:[20]

$$S = \frac{1-(r/r_0)^6}{1-(r/r_0)^{12}} \quad (1)$$

where r is the distance between the two chosen atom types and r_0 was 1.32 Å in the case of nitrogen–hydrogen and oxygen–hydrogen coordination number and 2.9 Å in the case of oxygen–carbon coordination number.

Protonation state of the cytosine/guanine radical pair cation: The coordinates of interest are the coordination number of hydrogen with respect to N^1 and N^2 of $G^{\bullet+}$ and the N^4 of cytosine.

In Figure 2c the free energy surfaces as a function of the guanine N^1 and cytosine N^4 hydrogen coordination number computed with the QM/MM partition of model A is reported. As a reference, we repeated the same calculation with the hydrogen-bonded radical base pair in gas phase (Figure 2b).

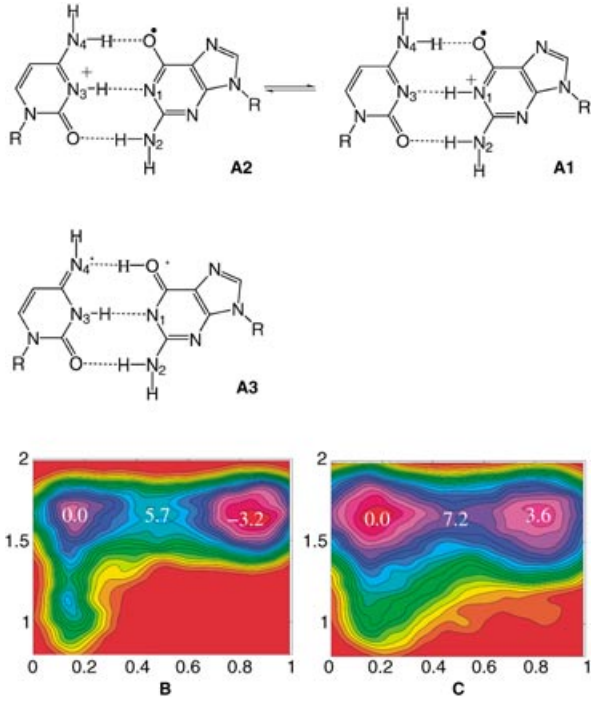

Figure 2. Free energy surfaces (in kcal mol^{-1}) of the N^1 (x) and N^4 (y) hydrogen coordination number (A) in gas phase (B) and in the fully hydrated DNA molecule (C). In A) the schematic representations of the protonation states are spatially arranged to match the corresponding minima in B and C. The surfaces B and C were obtained with 1347 and 2262 Gaussians with a height and width of 0.62 and 0.05 kcal mol^{-1} (see ref. [20]). The Gaussians were added each 50 steps of ab initio MD giving a total simulation time of 16.4 and 9.8 ps. The fictitious mass and the coupling constant of the restraints was set to 70 amu and 0.3, respectively. Since the free energies are defined modulo an undetermined constant we have chosen our zero to coincide with state 2.

The ΔE of the two minima in gas phase is $\approx$3 kcal mol^{-1} and the barrier is $\approx$6 kcal mol^{-1}, consistent with previous calculations.[42,43] The same energy differences, within a fraction of kcal mol^{-1}, are found by repeating the calculations with the HCTH functional. The ΔE calculations were repeated in the fully hydrated DNA within the QM/MM framework (model A of Figure 3 was used for the quantum subsystem, see also Supporting Information).

A remarkable inversion of stability takes place and we find that protomer A2 is stabilized by $\approx$4 kcal mol^{-1} with respect to A1 (Figure 2c); the other possible protonation state described by our choice of collective coordinates (A3, Figure 2) turns out to be energetically unfavorable.

This relative protonation stability inversion is remarkable not only because it is different from the gas phase results but also because it contradicts the hypothesis that the reaction toward 8-oxo-G (the main product found in double helical DNA) has to go through a $G^{\bullet+}$ intermediate. It is therefore essential to check the validity of the calculations. To this effect we have performed several geometry optimization energy calculations both in gas phase and in the DNA, at various levels of approximation and concluded that the errors were within the accuracy of the method (see Supporting Information).

We are now in a position to trace with confidence the origin of the protomer stability inversion. Further calculations were made on model A starting from the optimized structure. The role of the charges of the backbone and of the nearby sandwiching bases was studied by selectively switching them off. One set of geometry optimization/energy calculation was repeated leaving only the charges of the deoxyribose and phosphate attached to the quantum system and setting to zero all the other classical charges. The resulting ΔE value was -5.3 kcal mol^{-1}. A second set of geometry optimization/energy calculation was made with pure mechanical coupling between the classical and the quantum system, resulting in $\Delta E = -1.2$ kcal mol^{-1}. This analysis shows that the main sources of the energy reversal are the electrostatic coupling with the directly attached sugar and phosphate, the changes of geometry experienced by the bases going from gas phase to DNA and the dynamical fluctuations of the DNA backbone. On the other hand, electrostatic coupling with the remaining atoms including the nearby sandwiching bases has in this case little influence.

Formation of 8-hydroxy-7,8-dihydroguanyl radical: When the 8-hydroxy-7,8-dihydroguanyl radical (8-OH-G$^\bullet$) is formed from the $G^{\bullet+}$ (see Figure 4 top), the first step is a nucleophilic attack on G–C^8.[9] Therefore we chose as collective variables the oxygen coordination number of the G–C^8 and the hydrogen coordination number of water molecules (the model used was B, Figure 3). Moreover, since the protonation state can be expected to affect the reaction mechanism, we also include in the collective coordinate space the hydrogen coordination number of guanine N^1.

In Figure 4 we represent the events leading to the water addition to $G^{\bullet+}$. A total of 1950 steps of metadynamics for a total of 2.3 ps were made with model B (Figure 3). The tra-

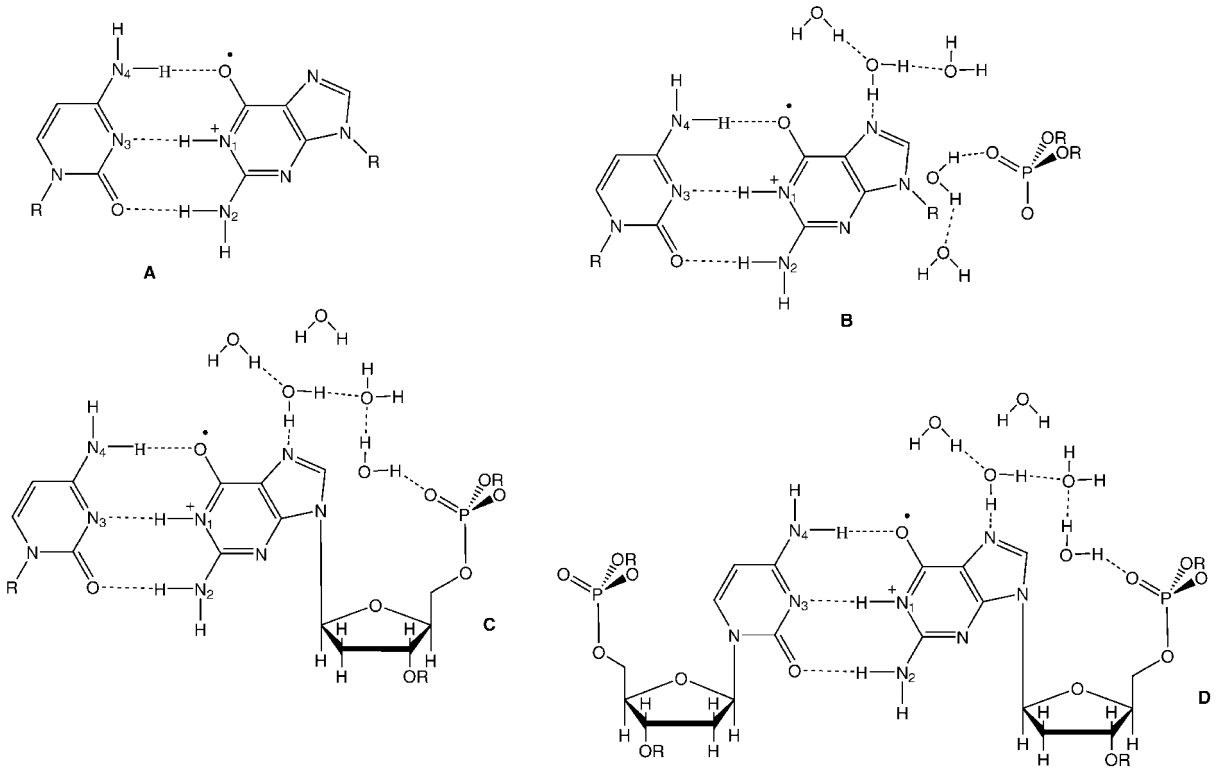

Figure 3. Quantum subsystems used in the QM/MM calculations. The smallest QM system (A) includes a G:C hydrogen-bonded pair linked with a classical bond between the deoxyribose C_1' and the nitrogen of the bases. Model B includes system A plus four water molecules and a phosphate anion. In model C the deoxyribose attached to the guanine is added to model B. In model D also the sugar and the phosphate attached to the cytosine are included.

jectory in the metacoordinate space is represented in Figure 4, middle. The system oscillates between state B ($G^{\bullet+}$) and state A (G(-H)$^{\bullet}$) for a long time until it has acquired enough energy to overcome the main barrier, which turns out to be water protolysis, as experimentally proved elsewhere for a similar system.[44] The barrier for this rate limiting step is $\approx$10–15 kcal mol^{-1}, consistently with the experimentally determined rate for the water addition to the $G^{\bullet+}$:C in DNA (6×10^4 s^{-1}).[45]

After the water dissociates, the hydroxide reacts almost immediately with the G, and the proton jumps back from C-N^3 to the G-N^1. Single point calculations on the couples 8-OH-G$^{\bullet}$:C and 8-OH-G(-H)$^{\bullet}$:C(H)$^+$ show that the first is more stable by as much as 22 kcal mol^{-1}. The steps that follow the formation of the radical 8-OH-G$^{\bullet}$ (Figure 4) and lead to the production in oxidizing conditions[46] of 8-oxo-G are well understood and will not be studied here.[1]

According to our calculations, the autoprotolysis of a water molecule close to $G^{\bullet+}$ is very significantly enhanced with respect to pure water. In order to understand the origin of this effect we performed some further analysis. The fraction of unpaired electron on each atom was calculated as the difference $\rho_{up}-\rho_{down}$ integrated around each atom up to a distance equal to the VdW radius. For comparison on the other QM water molecules it amounts to less than 1×10^{-4}, while it amounts to 0.2 electrons on the most radical atoms (i.e., C_4, C_5 and C_8).

We first considered $G^{\bullet}-H_2O$ pair in the gas phase in the same geometry as in the QM/MM simulation, and found that there is a small but significant charge transfer from the water HOMO to G$^{\bullet}$: 0.2×10^{-2} electrons (Figure 5b). This transfer is enhanced if we add the phosphate anion to the $G^{\bullet}-H_2O$ pair, 0.7×10^{-2} electrons (Figure 5c). Even larger is the charge transfer if we include in the calculation the effect of the full DNA environment by means of the QM/MM simulation: 1.2×10^{-2} electrons (Figure 5a). A study conducted on a number of full QM snapshots showed that this effect is general and the charge transfer is a function of the water G distance and the extent of radical localization on the G. Given the tendency of BLYP functional to delocalize the charge, we have repeated the gas phase calculations with the more accurate B3LYP functional and obtained the same results (Figure 5c, d) Even a CCSD calculation with a 6-31G* Gaussian basis set on the larger cluster (Figure 5c) supported our findings. The observed charge transfer does affect considerably the barrier of the protolysis reaction ($H_2O+(RO)_2PO_2^-HO^-+(RO)_2PO_2H$) which we calculated to be in the gas phase $\approx$41 kcal mol^{-1} and is reduced by the presence of the G$^{\bullet}$ to 25 kcal mol^{-1}. The full DNA environment stabilizes the transition state by another $\approx$10 kcal mol^{-1}.

A relevant question is whether our model is representative of real life biological DNA or whether the role of the phosphate is amplified by our use of a tightly packed crystal structure. In particular in our simulations a crucial role is

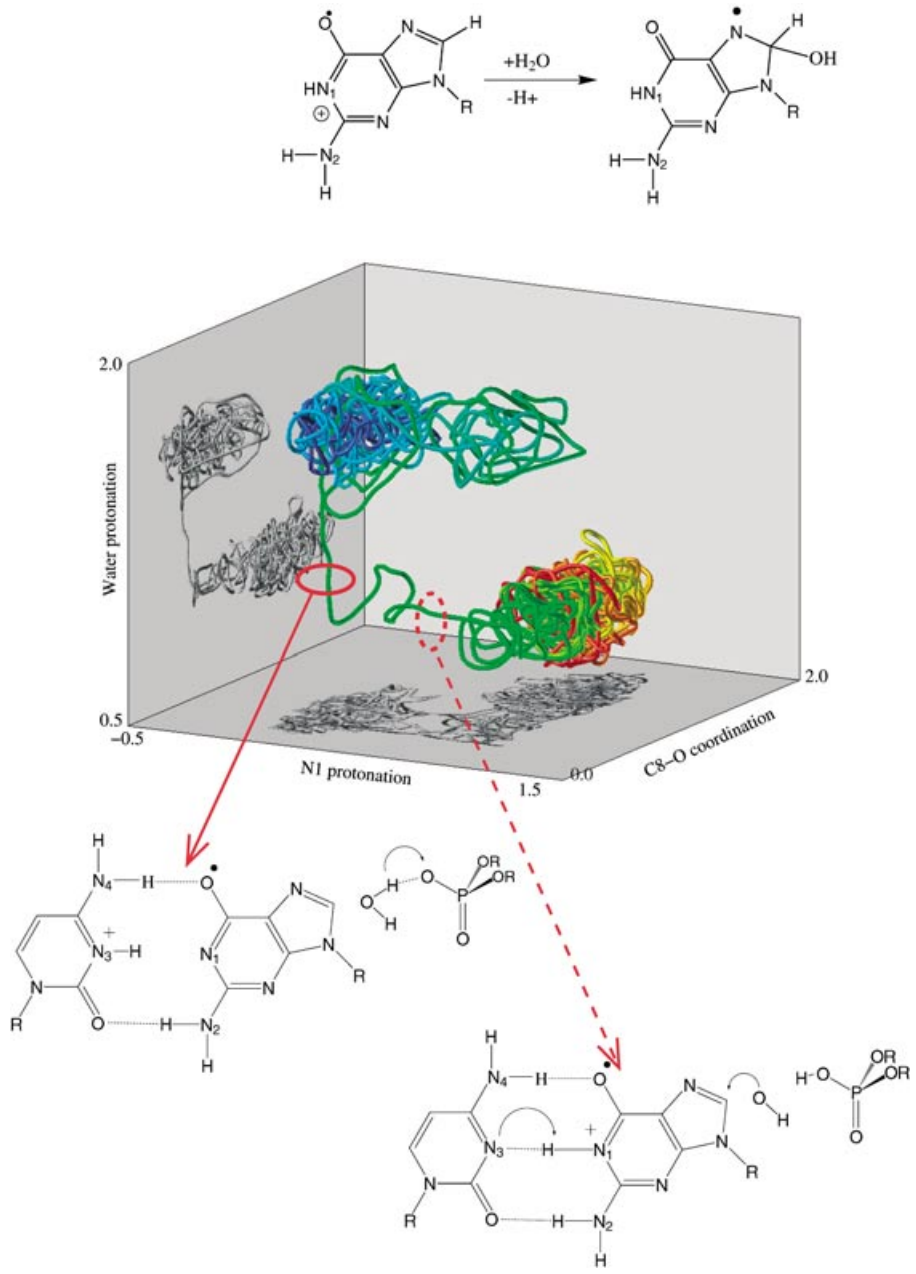

Figure 4. Conversion of $G^{\bullet+}$ to the 8-OH-$G^{\bullet}$ (top); 8-oxo-G is formed from this radical by further oxidation. Middle: trajectory of the reaction metadynamics in the 3D space of the collective coordinates: number of hydrogen atoms coordinating N^1 (x), number of oxygen atoms coordinating C^8 (y) and number of hydrogen atoms coordinating the water molecule closest to C^8 (z). The time evolution of the trajectory is color coded ranging from blue to red. The coordination numbers are defined as in Equation (1) with r_0 equal to 1.32, 1.32 and 2.9 Å respectively. The height and width of the added Gaussian potentials were 0.62 and 0.05 kcal mol^{-1}. The fictitious mass and the coupling constant of the restraints was set to 70 amu and 0.3, respectively. The continuous line encircles the rate limiting step of the reaction (water protolysis) while the dashed line encircles the hydroxide addition concerted with N^1 reprotonation step; the arrows show the corresponding transitions.

played by the phosphate of a neighboring strand. While in the chromosomes this kind of tightly packing might indeed occur, one needs to consider a more general case. We have therefore performed a simulation on the QM/MM model C of Figure 3. In this model the sugar and phosphate attached to the $G^{\bullet}$ are included in the QM part, while the closer phosphate of the neighboring strand is treated classically. Furthermore the effect of the latter phosphate on the QM part is excluded from the calculation. The outcome of this simulation is interesting. The barrier for the reaction is slightly increased by $\approx$3 kcal mol^{-1} and the proton is shuttled to the second nearest phosphate through a bridging water molecule via a Grotthuss mechanism. Since interstrand phosphate are always present and do not depend on the sequence, we believe that our mechanism is generally applicable.

Conclusion

The global picture arising from our calculations on the role played by the DNA structure on guanine oxidation is more complicated than previously thought and in some aspects even surprising. Our calculations in gas phase are in excellent agreement with the results found in the literature[16,42,43] that predict the pair $G^{\bullet+}$:C to be more stable than $G(-H)^{\bullet}$:$C(H)^{+}$. But in the hydrated DNA the electrostatics of the backbone as well as the different geometrical structure assumed by the pair lead to a reversal of the situation, and we find that in DNA $G(-H)^{\bullet}$:$C(H)^{+}$ is more stable by as much as 4–5 kcal mol^{-1}.

The rate limiting step of the 8-OH-$G^{\bullet}$ formation is the water autoprotolysis. Once the hydroxide is formed it promptly reacts with the $G^{\bullet+}$ and the proton jumps back on guanine N^1. This finding confirms speculations on the importance of DNA structure in changing the products of guanine oxidations. It was suggested that the differences in the products obtained in solution and in DNA are due to guanine stacking and pairing with cytosine. We found that stacking does not play a fundamental role in this case, while it could affect the competing reaction with O_2 by steric hindrance.[47] A fundamental role is instead played by the phosphate backbone, which reduces the barrier for the water protolysis by enhancing the charge transfer from $G^{\bullet}$ to the water and shuttles the lost proton to the water solution.

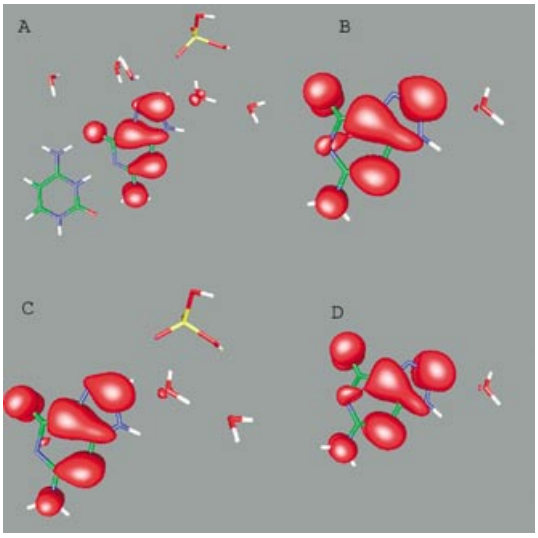

Figure 5. View of the three-dimensional structure of the G:C dimer and of the spin density isosurface (in red) associated with the radical cation state a) in the QM/MM calculation, b) in a cluster calculation (BLYP/plane waves) functional, c) in a cluster calculation including phosphate and a second water molecule (B3LYP6-31+G** basis set) and d) the same cluster as in b) except that the calculation was carried out in the B3LYP6-31+G** basis set framework. In a) water molecules, counterions and hydrogen atoms have been removed for clarity. All the isosurfaces represented have a value of 10^{-3} electrons $Å^{-3}$. From the Figure the effect of local environment (especially phosphate) in enhancing the charge transfer from the G$^{\bullet}$ to the water molecule is clear: passing from a) to b) the charge transfer is diminished by one order of magnitude. The same effect is confirmed in the calculation made with B3LYP and a Gaussian basis set: c) and d) and using the same cluster of c) at an higher level of theory (CCSD, not shown in the picture). In the full quantum calculation (not shown) whenever a water is closer than 5 Å to a G$^{\bullet}$ base a charge transfer can be appreciated.

This result confirms previous speculations[48] and could be checked by examining the G oxidation in a DNA:PNA duplex in which one strand would be incapable of catalyzing the deprotonation of water, or in a modified DNA were the phosphate backbone is changed in thiophosphate. Both experiments are feasible and it would be very interesting to see them performed. Indirect evidence for the relevance of the catalysis of the phosphate comes from two experiments.

Once the 8-OH-G$^{\bullet}$ is formed, the deprotonation of N^1 is impossible since the protonated form is more stable by more than 20 kcal mol^{-1}. So the overall role of the pairing of guanine with cytosine and the backbone in the oxidation reaction is quite subtle: first cytosine takes the proton from guanine radical cation, stabilizing even more the radical on the guanine (and localizing it), but then, once the backbone has catalyzed the hydroxide formation, the pairing favors the 8-OH-G$^{\bullet}$ formation by releasing the proton when needed and greatly stabilizing the product of the reaction. Fluctuations in the structure of the backbone also seem to play a role in aiding proton transfer from one base to the other. Overall we find evidence of a fine-tuned mechanism that acts in double helical DNA to funnel the oxidation reaction toward 8-oxo-G formation.

Acknowledgement

We thank A. Stirling and J. VandeVondele for useful discussions and J. M. Favre for the realization of some of the pictures. We acknowledge a generous grant from the Leibniz-Rechenzentrum/München on the Hitachi SR8000 supercomputer which made this calculation possible.

[1] C. Chatgilialoglu, P. O'Neil, *Exper. Geront.* **2001**, *36*, 1459–1471.
[2] C. G. Fraga, M. K. Shigenaga, J. W. Park, P. Degan, B. N. Ames, *Proc. Natl. Acad. Sci. USA* **1990**, *87*, 4533–4537.
[3] E. C. Friedberg, G. C. Walker, W. Siede, *DNA Repair Mutagenesis*, ASM Press, **1995**.
[4] S. Steenken, *Chem. Rev.* **1989**, *89*, 503–520.
[5] I. Saito, M. Takayama, H. Sugiyama, K. Nakatani, A. Tsuchida, M. Yamamoto, *J. Am. Chem. Soc.* **1995**, *117*, 6406–6407.
[6] H. Sugiyama, I. Saito, *J. Am. Chem. Soc.* **1996**, *118*, 7063–7068.
[7] Y. Yoshioka, Y. Kitagawa, Y. Takano, K. Yamaguchi, T. Nakamura, I. Saito, *J. Am. Chem. Soc.* **1999**, *121*, 8712–8719.
[8] F. Prat, K. N. Houk, C. S. Foote, *J. Am. Chem. Soc.* **1998**, *120*, 845–846.
[9] C. J. Burrows, J. G. Muller, *Chem. Rev.* **1998**, *98*, 1109–1151.
[10] In fact, there is mounting evidence that vacancies can travel very long distances in double helical DNA[12,49,50] and concentrate on G.[13]
[11] B. Giese, *Curr. Opin. Chem. Biol.* **2002**, *6*, 612–618.
[12] B. Giese, *Annu. Rev. Biochem.* **2002**, *71*, 51–70.
[13] B. Giese, *Acc. Chem. Res.* **2000**, *33*, 631–636.
[14] P. T. Henderson, D. Jones, G. Hampikian, Y. Kan, G. B. Schuster, *Proc. Natl. Acad. Sci. USA* **1999**, *96*, 8353–8358.
[15] C. Wan, T. Fiebig, S. O. Kelley, C. R. Tradway, J. K. Barton, A. Zewail, *Proc. Natl. Acad. Sci. USA* **1999**, *96*, 6014–6019.
[16] J. Reynisson, S. Steenken, *Phys. Chem. Chem. Phys.* **2002**, *4*, 527–532.
[17] P. Hobza, J. Sponer, *Chem. Rev.* **1999**, *99*, 3247–3276.
[18] F. L. Gervasio, P. Carloni, M. Parrinello, *Phys. Rev. Lett.* **2002**, *89*, 108102/1–4.
[19] R. N. Barnett, C. L. Cleveland, A. Joy, U. Landman, G. Schuster, *Science* **2001**, *294*, 567–571.
[20] A. Laio, M. Parrinello, *Proc. Natl. Acad. Sci. USA* **2002**, *99*, 12562–12566.
[21] M. Iannuzzi, A. Laio, M. Parrinello, *Phys. Rev. Lett.* **2003**, *90*, 238302.
[22] A. Laio, J. VandeVondele, U. Roethlisberger, *J. Chem. Phys.* **2002**, *116*, 6941–6947.
[23] L. P. Candeias, S. Steenken, *J. Am. Chem. Soc.* **1989**, *111*, 1094–1099.
[24] K. Hildebrand, D. Schulte-Frohlinde, *Free Radical Res. Commun.* **1990**, *11*, 195–206.
[25] C. J. Mundy, M. E. Colvin, A. A. Quong, *J. Phys. Chem. A* **2002**, *106*, 10063–10071.
[26] S. Steenken, *Biol. Chem.* **1997**, *378*, 1293–1297.
[27] S. Steenken, *Free Radical Res. Commun.* **1992**, *16*, 349–379.
[28] T. Douki, J. L. Ravanat, D. Angelov, J. R. Wagner, J. Cadet, *Top. Curr. Chem.* **2004**, *236*, 1–25.
[29] J. Cadet, *DNA Adducts: Identificarion and Biological Significance*, IARC Scientific, **1994**.
[30] T. Douki, D. Angelov, J. Cadet, *J. Am. Chem. Soc.* **2001**, *123*, 11360–11366.
[31] D. Angelov, A. Spassky, M. Berger, J. Cadet, *J. Am. Chem. Soc.* **1997**, *119*, 11373–11380.
[32] L. P. Candeias, S. Steenken, *Chem. Eur. J.* **2000**, *6*, 475–484.
[33] W. Luo, J. G. Muller, E. M. Rachlin, C. J. Burrows, *Chem. Res. Toxicol.* **2001**, *14*, 927–938.
[34] C. Ban, B. Ramakrishnan, M. Sundaralingam, *Biophys. J.* **1996**, *71*, 1215–1221.
[35] W. Saenger, *Principles of Nucleic Acid Structure*, Springer, **1984**.
[36] In the QM/MM simulations the two subsystems are electrostatically and mechanically coupled as described in ref. [22] The quantum system was terminated at the QM/MM boundary with hydrogen atoms saturating the valence of the boundary atoms. Since these added hydrogen atoms must interact with the quantum but not with

the classical sub-system, their electrostatic interaction with the nearby classical atoms was shielded in order to avoid the formation of unphysical hydrogen bonds with the nearby classical atoms. To that end, the MM atoms covalently connected to QM atoms are coupled with the quantum system by a Coulomb potential with a set of ESP-like charges, localized on the QM atoms and defined as described in ref. [51]. In this manner, pair interactions that have to be shielded can be explicitly excluded from the interaction Hamiltonian.

[37] The functional of choice for most calculations was the BLYP functional.[52,53] Since it was suggested that other "pure" functionals (e.g. HCTH[54,55]) give better results than BLYP for deprotonation and transition state energies,[55] in a few cases we repeated the calculations with that functional, but the energy differences that we obtained for our system were well within the error bar.[55] The Kohn–Sham orbitals were expanded up to an energy cutoff of 70 Ry and the calculations were made in the local spin density framework (i.e., singly occupied orbitals). The classical region that included all the remaining atoms was treated with the Amber force field.[56]

[38] N. Troullier, J. L. Martins, *Phys. Rev. B* **1991**, *43*, 1993–2006.

[39] *CPMD*, Copyright IBM Corp 1990–2001, Copyright MPI fuer Festkoerperforschung Stuttgart, **1997–2001**.

[40] A. Laio, F. L. Gervasio, J. VandeVondele, M. Sulpizi, U. Rothlisberger, *J. Phys. Chem. B* **2004**, *108*, 7963–7968.

[41] M. Sprik, *Faraday Discuss.* **1998**, *110*, 437–445.

[42] M. Hutter, T. Clark, *J. Am. Chem. Soc.* **1996**, *118*, 7574–7577.

[43] A. O. Colson, B. Besler, M. D. J. Sevilla, *J. Phys. Chem.* **1992**, *96*, 9787–9794.

[44] M. Oyama, K. Nozaki, T. Nagaoka, S. Okazaki, *Bull. Chem. Soc. Jpn.* **1990**, *63*, 33–41.

[45] Assuming $\tau \approx 1$.

[46] In reducing conditions this precursor is converted into 2,6-diamino-4-hydroxy-5-formamidopyrimidine nucleoside (FapyG).[1]

[47] Calculations on this alternative oxidation pathway are in progress and preliminary results indicate the existence in DNA of a barrier to oxygen attack due to steric hindrance posed by neighboring bases.

[48] E. Meggers, M. E. Michel-Beyerle, B. Giese, *J. Am. Chem. Soc.* **1998**, *120*, 12950–12955.

[49] U. VonBarth, L. Hedin, *J. Phys. C* **1972**, *5*, 1629–1642.

[50] Starting from 300 K the temperature was cooled down to 2 K, rescaling the velocities by a factor of 0.99 each step. This procedure, while ensuring convergence to a local minimum, generally does not allow for major rearrangements of the structure. However in this case we started from a geometry that was already optimized and whose close packing of the atoms taken from the X-ray crystal structure[34] does not allow much rearrangement of the backbone.

Received: February 19, 2004
Published online: August 20, 2004

